CHEMISTRY OF MATERIALS

ARTICLE

pubs.acs.org/cm

Mechanism of Sulfur Incorporation into Solution Processed $CuIn(Se,S)_2$ Films

Choong-Heui Chung, Bao Lei, Brion Bob, Sheng-Han Li, William W. Hou, Hsin-Sheng Duan, and Yang Yang*

California NanoSystems Institute and Department of Materials Science and Engineering, University of California Los Angeles, Los Angeles, California 90095, United States

ABSTRACT: We have investigated the incorporation of sulfur into $CuIn(Se,S)_2$ thin films from different bonding environments in hydrazine-based precursor solutions. Sulfur is present in the form of $(N_2H_5)_2S$, $[Cu_6S_4]^{2-}$, and $[In_2(Se,S)_4]^{2-}$ complexes in mixed $CuIn(Se,S)_2$ precursor solutions. On the basis of compositional information from the precursor solutions and annealed films, we find that the incorporation efficiency of sulfur from $(N_2H_5)_2S$ into the final film is extremely low as a result of the high volatility of this compound and its weak interaction with other species while in solution. Using the same methodology, we additionally report that approximately 80% of the sulfur from $[In_2(Se,S)_4]^{2-}$ is incorporated into the final material, compared to approximately 40% of the sulfur from $[Cu_6S_4]^{2-}$ complexes. This difference in sulfur incorporation efficiency may be due to the relatively weak Cu−S bonds present in the $[Cu_6S_4]^{2-}$ structure, which are somewhat unstable compared to the In−S bonds in the $[In_2(Se,S)_4]^{2-}$ complex. This method makes it possible to precisely control the sulfur content in $CuIn(Se,S)_2$ films by adjusting the S/Se ratio of the $[In_2(Se,S)_4]^{2-}$ ions in the final precursor solution. These results will enable the precise adjustment and optimization of the energy band gap in solution-processed $CuIn(Se,S)_2$ absorber layers for the future fabrication of improved photovoltaic devices.

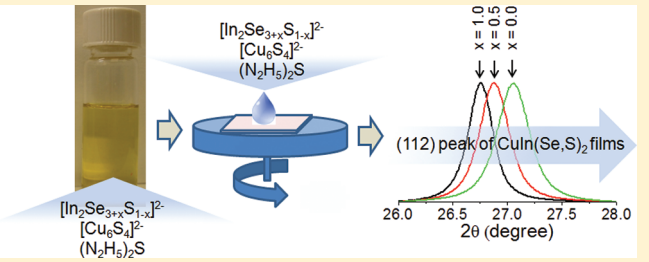

KEYWORDS: solar cells, $CuIn(Se, S)_2$, band gap, hydrazine, molecular precursors

INTRODUCTION

$CuInSe_2$ and its alloys have been extensively investigated as some of the most promising absorber materials for thin film photovoltaic device applications, owing to a high optical absorption coefficient, structural tolerance to large changes in material stoichiometry, and a tunable electronic band gap.[1] Band gap optimization is typically achieved by partially replacing indium or selenium with gallium or sulfur, respectively. $Cu(In,Ga)Se_2$ thin film solar cells with efficiencies of roughly 20% have been reported through the use of the vacuum processing techniques in the deposition of the absorber layer.[2] However, these techniques introduce challenging issues for the low-cost production of large area modules as a result of the processing complexities associated with vacuum-based device fabrication.[3,4] Thus, non-vacuum deposition techniques have been extensively pursued for more than a decade in an attempt to overcome these issues.[5−8]

Hydrazine solution processing has demonstrated $CuInSe_2$-based thin film solar cells with efficiencies of up to 13.6% despite the early developmental stage of this technique.[9] While this approach can readily be used to incorporate gallium into the deposited films,[10−12] hydrazine-processed $CuIn(Se,S)_2$ layers are almost completely devoid of sulfur, often despite the addition of excess sulfur to the precursor solutions. W. Liu et al. have reported hydrazine solution-processed $CuIn(Se,S)_2$ films with sulfur content up to approximately 15 atomic %,[13] but the detailed mechanism of sulfur incorporation into the films during the formation of the chalcopyrite phase from liquid precursors remains largely undetermined. Precise control over the sulfur content of $CuIn(Se,S)_2$ and $Cu(In,Ga)(Se,S)_2$ thin films is essential in order to facilitate the optimization of the energy band gap and to produce any desired band gap grading. Thus, a deeper understanding of the incorporation mechanism of dissolved sulfur into deposited $CuIn(Se,S)_2$ absorber layers represents a significant asset to the further improvement of hydrazine-processed device performance. In this report, we investigate the mechanism of sulfur incorporation into hydrazine solution-processed $CuIn(Se,S)_2$ films prepared using precursor solutions containing the complexes $(N_2H_5)_2S$, $[Cu_6S_4]^{2-}$ and $[In_2(Se,S)_4]^{2-}$.

EXPERIMENTAL SECTION

The solutions employed in this investigation consisted of elemental sulfur, Cu_2S precursor, $In_2(Se,S)_3$ precursor, and the combined $CuIn(Se,S)_2$ precursor mixture, all dissolved in anhydrous hydrazine. ***Caution:*** *hydrazine is highly toxic and should be handled with appropriate protective equipment to prevent contact with both the liquid and the vapor.* The elemental sulfur solution was prepared by dissolving the desired

Received: June 27, 2011
Revised: October 4, 2011
Published: October 17, 2011

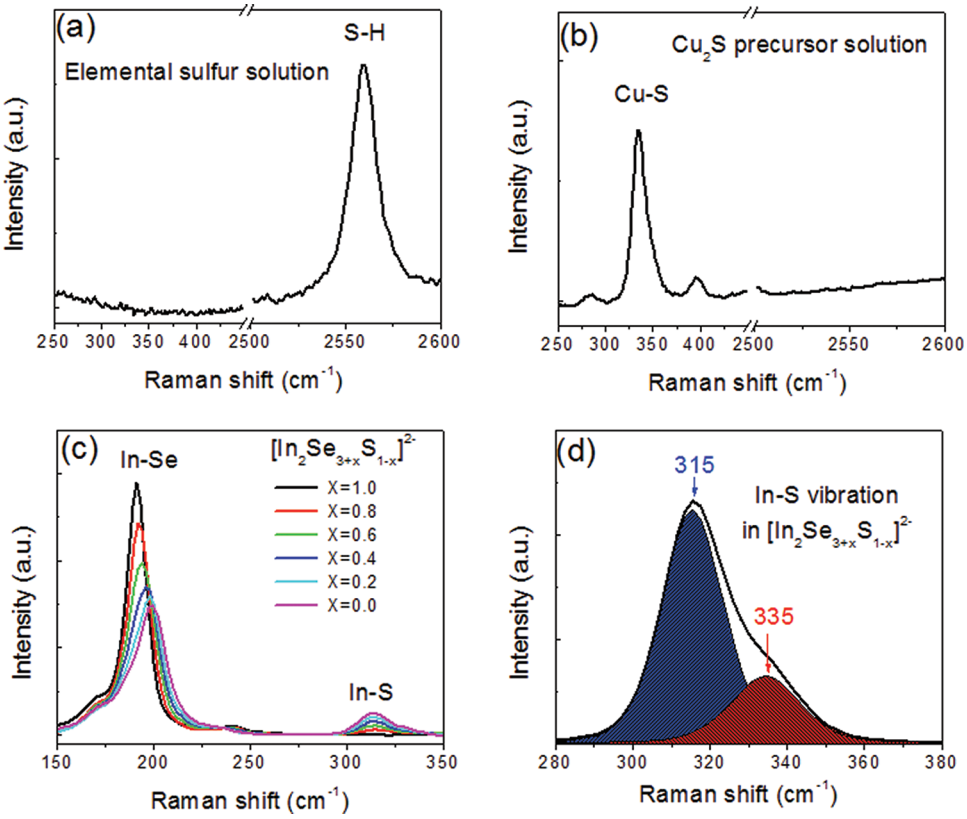

Figure 1. Raman spectra of (a) elemental sulfur solution, (b) Cu_2S precursor solution having a Cu_2S/S ratio of 3, (c) $In_2(Se,S)_3$ precursor solutions containing an equal amount of elemental chalcogen (Se and S) and In_2Se_3, with various amounts of selenium and sulfur, and (d) deconvolution of the In−S peaks obtained from the $In_2(Se,S)_3$ precursor solution.

quantity of elemental sulfur powder in hydrazine. To prepare the Cu_2S precursor solution, Cu_2S powder was combined with elemental sulfur in hydrazine, with the Cu_2S/S molar ratio adjusted to 3 in all cases. To prepare the $In_2(Se,S)_3$ precursor solutions, In_2Se_3 was combined with elemental selenium and elemental sulfur in hydrazine, with the total amount of chalcogen (combined S and Se) set equal to that of In_2Se_3. Each solution was stirred for more than one week at room temperature. To prepare the final $CuIn(Se,S)_2$ precursor solutions, the Cu_2S precursor solution was combined with the $In_2(Se,S)_3$ precursor solution. Additionally, extra sulfur solution was added to adjust the $S/(S + Se)$ ratio to the same value in each of the final $CuIn(Se,S)_2$ solutions. All solution preparation and film deposition took place inside an N_2 filled drybox with water and oxygen levels each below 1 ppm. The $CuIn(Se,S)_2$ solutions were then spun onto SiO_2-coated silicon substrates, followed by a thermal annealing step at 350 °C for 30 min to form a polycrystalline film. These films were then characterized using Raman spectroscopy, X-ray diffraction (XRD), and energy dispersive X-ray (EDX) spectroscopy. Films with thicknesses of approximately 1 μm were prepared on Mo-coated glass substrates for photoluminescence (PL) measurements by repeating the spin coating and annealing process six to eight times.

Raman spectroscopy was performed on the precursor solutions and $CuIn(Se,S)_2$ thin films in a confocal backscattering configuration at room temperature using a Renishaw InVia model with a 514.5 nm argon laser as a light source. Prior to measurement, each solution was sealed by placing vacuum grease between a cavity slide and a thin cover slide while inside an N_2 filled drybox to reduce the possibility of chemical changes in solution due to exposure to oxygen and moisture. The laser power was adjusted to 10 mW and 1 mW when measuring solutions and thin films, respectively. The laser beam size was approximately 10 and 1 μm for precursor solutions and films, respectively. XRD characterization was performed on the annealed films using a PANalytical X'Pert Pro X-ray diffractometer with a Cu Kα radiation source beam. The compositions of the thin films were obtained using EDX spectroscopy within an FEI Quanta 600 scanning electron microscope at an acceleration voltage of 5 kV. Each EDX spectrum was obtained from an area of 100 μm × 100 μm on the sample surface. FeS_2, copper, selenium, and InAs were used as standards for the analysis of the sulfur, copper, selenium, and indium content of the films during EDX measurements. Room temperature PL spectra were obtained to estimate the band gap of the $CuIn(Se,S)_2$ films using a Horiba Fluorolog-3 spectrometer with a 660 nm semiconductor laser as the excitation source. The PL signal from the samples was detected by a Hamamatsu H10330A photomultiplier tube cooled to −60 °C during operation.

RESULTS AND DISCUSSIONS

Knowledge of the specific sulfur-containing molecular species present in hydrazine precursor solutions is essential to investigate the effectiveness of sulfur incorporation into hydrazine-processed $CuIn(Se,S)_2$ films. It has been reported that elemental sulfur dissolves in hydrazine to form the $(N_2H_5)_2S$ compound, and Cu_2S dissolves in hydrazine in the presence of additional sulfur to form $[Cu_6S_4]^{2-}$ complexes.[14] Figure 1 shows typical Raman spectra of (a) the elemental sulfur solution and (b) the Cu_2S precursor solution with a Cu_2S/S ratio of 3. The distinct peak located at 2560 cm^{-1} can be assigned to an S−H stretching vibrational mode of $(N_2H_5)_2S$, and the peak located at 335 cm^{-1} can be assigned to a Cu−S stretching mode of the $[Cu_6S_4]^{2-}$ ions. More detailed analysis can be found elsewhere.[14]

dx.doi.org/10.1021/cm201827c |*Chem. Mater.* 2011, 23, 4941–4946

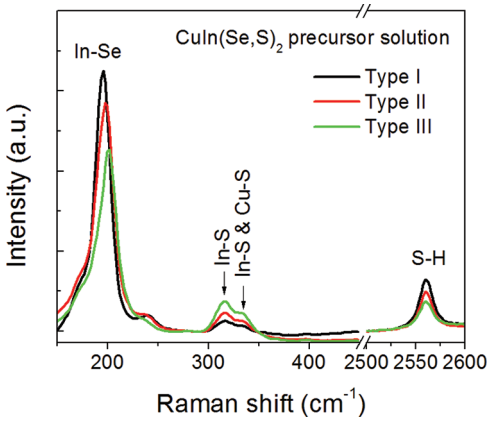

Figure 2. Raman spectra of three different types of $CuIn(Se,S)_2$ precursor solutions, each with an S/(Se + S) ratio of 0.6.

The $[In_2Se_4]^{2-}$ complexes can be formed by mixing equal amounts of In_2Se_3 and elemental selenium in hydrazine.[14] In our precursor solutions, we make use of $[In_2Se_{3+x}S_{1-x}]^{2-}$, or more simply $[In_2(Se,S)_4]^{2-}$, ions by partially or fully replacing elemental selenium with elemental sulfur when dissolving the initial material. Figure 1c shows the Raman spectra of $In_2(Se,S)_3$ precursor solution containing an equal amount of elemental chalcogen (Se and S) and In_2Se_3 as a function of the amount of sulfur substituted for selenium. It clearly exhibits a strong peak in the range 192−200 cm^{-1}, which can be attributed to the In−Se bond vibration of the indium chalcogenide complex.[15−17] The peak corresponding to this vibrational mode progressively shifts toward higher energies with increasing replacement of selenium by sulfur atoms in the precursor solutions. In addition, the intensities of In−S peaks, which can be deconvoluted into two peaks located at 315 cm^{-1} (main peak) and 335 cm^{-1} (secondary peak), were substantially enhanced by increasing the sulfur content in the precursor solutions, as shown in Figure 1d. Furthermore, the peaks corresponding to S−H bonds, which can result from the formation of $(N_2H_5)_2S$ molecules, was not detected because all the sulfur atoms in the In_2Se_3 solution are consumed to form $[In_2(Se,S)_4]^{2-}$, which is no longer capable of exhibiting an S−H vibration. Therefore, the dominant indium−selenium−sulfur phase present in hydrazine solutions must be $[In_2(Se,S)_4]^{2-}$, which is formed through the following the overall chemical equation:

$$2In_2Se_3 + 2xSe + 2(1-x)S + 5N_2H_4 \rightarrow 2[In_2Se_{3+x}S_{1-x}]^{2-} + 4N_2H_5^{+} + N_2(g) \quad (1)$$

The stoichiometry of the $[In_2Se_{3+x}S_{1-x}]^{2-}$ complex can be easily adjusted by varying the elemental sulfur and selenium initially added to the solutions.

To investigate of sulfur incorporation efficiency from each molecular species into final $CuIn(Se,S)_2$ films, three specific $[In_2(Se,S)_4]^{2-}$ complexes, $[In_2Se_4]^{2-}$, $[In_2Se_{3.5}S_{0.5}]^{2}$, and $[In_2Se_{3.0}S_{1.0}]^{2-}$, were prepared. The Cu_2S precursor solutions were mixed with each of the three $In_2(Se,S)_3$ solutions to prepare three distinct $CuIn(Se,S)_2$ solutions. Type I $CuIn(Se,S)_2$ precursor solution was prepared by combining $[Cu_6S_4]^{2-}$ with $[In_2Se_4]^{2-}$; Type II $CuIn(Se,S)_2$ precursor solution was prepared by combining $[Cu_6S_4]^{2-}$ with $[In_2Se_{3.5}S_{0.5}]^{2-}$; and Type III $CuIn(Se,S)_2$ precursor solution was prepared by combining $[Cu_6S_4]^{2-}$ with $[In_2Se_{3.0}S_{1.0}]^{2-}$. Appropriate amounts of $(N_2H_5)_2S$ solution were then added to adjust the S/(S + Se) ratio in the final $CuIn(Se,S)_2$ precursor solutions to the constant value of 0.6.

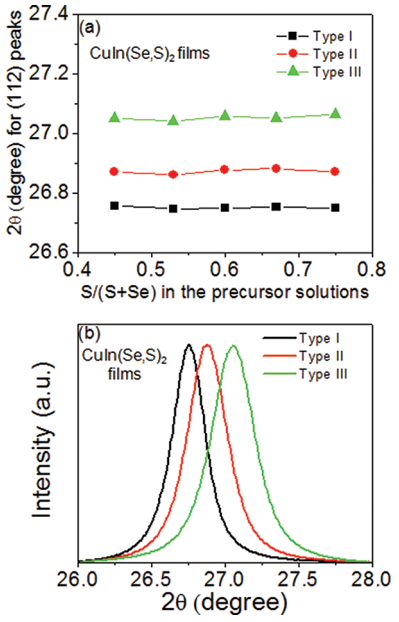

Figure 3. (a) Measured $2\theta_{112}$ values of $CuIn(Se,S)_2$ films prepared using three different types of $CuIn(Se,S)_2$ precursor solution as a function of the S/(Se + S) ratio in solution and (b) X-ray diffraction patterns of the (112) peak of $CuIn(Se,S)_2$ films prepared using three different types of $CuIn(Se,S)_2$ precursor solution.

Figure 2 shows the Raman spectra obtained from each Type of $CuIn(Se,S)_2$ solution with S/(S + Se) ratios set to 0.6. The peak intensity is normalized using the hydrazine peak intensity. After their initial mixing, solutions were stirred for 1 h before Raman characterization. The intensity of In−S originating from the $[In_2(Se,S)_4]^{2-}$ species gradually increases from Type I through Type III, while both the S−H bond intensity originating from $(N_2H_5)_2S$ and the In−Se bond intensity originating from $[In_2(Se,S)_4]^{2-}$ are gradually reduced. The increase of a peak located at 335 cm^{-1} is also originated from the increase of the secondary peak of the In−S bond in $[In_2(Se,S)_4]^{2-}$. In other words, a larger fraction of sulfur atoms are bonded to indium atoms in the form of $[In_2(Se,S)_4]^{2-}$ and fewer sulfur atoms are bonded to hydrogen atoms in the form of $(N_2H_5)_2S$, in the progression of Type I, Type II, and Type III.

$CuIn(Se,S)_2$ films were prepared by spin-casting each of the $CuIn(Se,S)_2$ solutions, followed by a thermal annealing step at 350 °C. Figure 3 shows the dependence of the diffraction angle 2θ of the (112) peak of the $CuIn(Se,S)_2$ films on the S/(Se + S) ratios in the precursor solutions. The sulfur to selenium ratio for each type of solution was controlled by varying the amount of $(N_2H_5)_2S$ added to the mixed $[Cu_6S_4]^{2-}$ and $[In_2(Se,S)_4]^{2-}$ solutions. Increased sulfur incorporation in the $CuIn(Se,S)_2$ phase would cause its lattice parameter to shift to lower values, resulting in larger 2θ values.[18] In this case, however, the $2\theta_{112}$ values of the $CuIn(Se,S)_2$ films were almost identical regardless of the S/(S + Se) ratio for each type of $CuIn(Se,S)_2$ precursor solution, as shown in Figure 3a. This indicates that the sulfur incorporation efficiency from the $(N_2H_5)_2S$ molecular species is negligible, even at relatively high concentrations within the $CuIn(Se,S)_2$ precursor solution.

dx.doi.org/10.1021/cm201827c |Chem. Mater. 2011, 23, 4941–4946

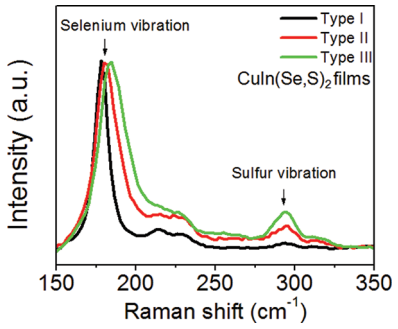

Figure 4. Raman spectra of $CuIn(Se,S)_2$ films prepared using three different types of $CuIn(Se,S)_2$ precursor solution.

Additionally, it has been shown that interaction between molecular species in hydrazine precursor solutions can affect their Raman shift peak intensities.[14] However, the peak intensity of the S−H bond originating from $(N_2H_5)_2S$ shows negligible change when the elemental sulfur solution is mixed with either or both of the Cu_2S and $In_2(Se,S)_3$ precursor solutions, indicating that $(N_2H_5)_2S$ interacts weakly or not at all with the metal chalcogenide anions. Thus, $(N_2H_5)_2S$ molecules that are only weakly coordinated with the nonvolatile metal chalcogenide precursors in the final precursor solution can be anticipated to evaporate during spin coating and the following thermal annealing step. This prediction is supported by the observation that a significant amount of sulfur is lost from the precursor films even at temperatures below 120 °C.[19]

In contrast, $CuIn(Se,S)_2$ films fabricated using $In_2(Se,S)_3$ precursor solutions with different amounts of sulfur substituted for selenium showed clearly different values of $2\theta_{112}$, as shown in Figure 3a and b. The $2\theta_{112}$ value of the $CuIn(Se,S)_2$ films gradually increased with increasing sulfur content in $[In_2(Se,S)_4]^{2-}$ ions in the precursor solutions, indicating that sulfur from $[In_2(Se,S)_4]^{2-}$ ions is efficiently incorporated into the films. In response to the inclusion of additional sulfur atoms into the $CuIn(Se,S)_2$ phase, the $2\theta_{112}$ value moves from 26.75° to 26.88° and 27.06° in the progression of Type I, II, and III precursor solutions. Using the empirical approximation for the tetragonal lattice parameters of the $CuInSe_xS_{2-x}$ phase, which are described by the following equations:[18]

$$a = 5.532 + 0.0801x + 0.0260x^2,$$
$$c = 11.156 + 0.1204x + 0.0611x^2 \quad (2)$$

the sulfur content of each $CuIn(Se,S)_2$ film can be estimated to be approximately 4.5, 8.5, and 14.5 atomic % for Type I, II, and III, respectively.

Raman spectra obtained from each of these films provides further evidence for this effect. The peak resulting from the oscillatory motion of selenium atoms with respect to their neighboring copper and indium atoms in chalcopyrite $CuInSe_2$ is typically reported at 174 cm^{-1}.[20,21] The corresponding peak in our spectra in Figure 4 is gradually shifted in energy with increasing sulfur content in the $[In_2(Se,S)_4]^{2-}$ precursor and is located at 178, 181, and 184 cm^{-1}, respectively, for each solution. Using the experimentally determined relationship between sulfur content and measured peak position,[22] the sulfur content in the $CuIn(Se,S)_2$ films was estimated to be approximately 5, 10, and 15 atomic % for Type I, II, and III, respectively. The estimated values of the sulfur content based on these Raman spectra are quite close to the values deduced using the (112) peak position obtained from XRD measurements. In addition, the sulfur vibrational mode in $CuIn(S,Se)_2$ located at 291 cm^{-1} shows increased intensity from Type I to Type III. These effects indicate that the sulfur content introduced into the annealed $CuIn(Se,S)_2$ films progressively increases in direct correlation with the sulfur content of the $[In_2(Se,S)_4]^{2-}$ precursor.

The compositional data discussed above now allows us to quantitatively estimate the efficiency of sulfur incorporation into the annealed $CuIn(Se,S)_2$ films prepared from solutions containing $[Cu_6S_4]^{2-}$ and $[In_2(Se,S)_4]^{2-}$. We propose the following chemical reaction for the formation of the $CuIn(Se,S)_2$ phase from $[Cu_6S_4]^{2-}$ and $[In_2(Se,S)_4]^{2-}$ molecular precursors:

$$[Cu_6S_4]^{2-} + 3[In_2(Se_{3+x}S_{1-x})]^{2-} + 8N_2H_5^{+} \rightarrow 6CuInSe_{(3+x)\eta/2}S_{2\varepsilon/3+(1-x)\zeta/2} + 3(3+x)(1-\eta)Se + (4(1-\varepsilon) + 3(1-x)(1-\zeta))S + 8N_2H_4 + 4H_2 \quad (3)$$

where η is the incorporation efficiency of selenium from the $[In_2(Se,S)_4]^{2-}$ species into the films and ε and ζ are the incorporation efficiencies of sulfur from the $[Cu_6S_4]^{2-}$ and $[In_2(Se,S)_4]^{2-}$ species, respectively. In this analysis, we have set the incorporation efficiency of copper and indium from their respective molecular precursors into the $CuIn(Se,S)_2$ phase to be unity. The left-hand side of the above equation represents the molecular species $[Cu_6S_4]^{2-}$ and $[In_2(Se,S)_4]^{2-}$ present in the $CuIn(Se,S)_2$ precursor solution. Although $(N_2H_5)_2S$ molecules are clearly present in the final precursor solution, we have not included them in the proposed chemical reaction because this species negligibly incorporates into the final films. We include $[N_2H_5]^+$ ions on the reactant side to maintain charge neutrality within the mixed solution. The first term on the right-hand side the equation is the $CuIn(Se,S)_2$ phase whose composition will be determined by the incorporation efficiency of chalcogen (S and Se) from the $[Cu_6S_4]^{2-}$ and $[In_2(Se,S)_4]^{2-}$ species, and the latter terms represent loss of excess chalcogen, hydrazine, and hydrogen during the coating and thermal annealing processes. In the proposed chemical equation, we assume that sulfur and selenium evaporate in the form of elemental vapor for the simplicity of the proposed reaction. Even if the chalcogen species that do not remain in the solid phase were to volatilize in other forms such, as H_2S and H_2Se, it would not change the calculated values for the incorporation efficiencies of each precursor molecule into the final film.

With a quantitative model in place, EDX spectroscopy was employed to more precisely determine the composition of the $CuIn(Se,S)_2$ films from three different solutions, and the results are listed in Table 1. The sulfur compositions calculated from the XRD and Raman spectra were used as accuracy standards, serving to double and triple check the measured EDX values, which showed good agreement at each film composition. The incorporation efficiencies of selenium from $[In_2Se_{3+x}S_{1-x}]^{2-}$ into the solid phase can be estimated at each x value because $[In_2(Se,S)_4]^{2-}$ is the only molecule containing selenium atoms in the mixed precursor solutions. However, two molecular precursors, $[Cu_6S_4]^{2-}$ and $[In_2Se_{3+x}S_{1-x}]^{2-}$, contain sulfur atoms, so that a combination of EDX data at two different x values is necessary to obtain incorporation efficiencies of sulfur from $[Cu_6S_4]^{2-}$ and $[In_2(Se,S)_4]^{2-}$ into the films. Approximately 40% of the sulfur atoms in $[Cu_6S_4]^{2-}$ are estimated to be incorporated into the annealed films, while approximately 80% of sulfur and 90% of selenium atoms from $[In_2(Se,S)_4]^{2-}$ are

dx.doi.org/10.1021/cm201827c |Chem. Mater. 2011, 23, 4941–4946

Table 1. EDX Results for the Composition of Annealed $CuIn(Se,S)_2$ Films Prepared Using Three Different Types of $CuIn(Se,S)_2$ Precursor Solution, Each with an S/(Se + S) Ratio of 0.6

	$CuIn(Se,S)_2$ precursor	$CuIn(Se,S)_2$				
type	molecules	[Cu] atomic %	[In] atomic %	[Se] atomic %	[S] atomic %	stoichiometry
I	$[Cu_6S_4]^{2-}$, $(N_2H_5)_2S$, $[In_2Se_4]^{2-}$	25.21	24.89	43.39	6.51	$CuInSe_{1.74}S_{0.26}$
II	$[Cu_6S_4]^{2-}$, $(N_2H_5)_2S$, $[In_2Se_{3.5}S_{0.5}]^{2-}$	24.8	25.22	38.19	11.79	$CuInSe_{1.53}S_{0.47}$
III	$[Cu_6S_4]^{2-}$, $(N_2H_5)_2S$, $[In_2Se_{3.0}S_{1.0}]^{2-}$	24.71	25.24	33.71	16.34	$CuInSe_{1.35}S_{0.65}$

Table 2. Incorporation Efficiency of Sulfur in $[Cu_6S_4]^{2-}$ and $[In_2(Se,S)_4]^{2-}$ and Selenium in $[In_2(Se,S)_4]^{2-}$ into Annealed $CuIn(Se,S)_2$ Films

Se	$x = 0.0$	$x = 0.5$	$x = 1.0$	ave	std
η^a(%)	90	87	87	88	1.7
S	$x = 0.0$, $x = 0.5$	$x = 0.5$, $x = 1.0$	$x = 1.0$, $x = 0.0$	ave	std
ε^b (%)	38	39	39	39	0.7
ζ^b (%)	73	84	79	79	5.5

[a] η is calculated based on the equation $(3 + x)\eta/2 = y$ in $CuInSe_yS_z$ [b] ε and ζ are calculated based on the equation $(2/3)\varepsilon + (1 - x)\zeta/2 = z$ in $CuInSe_yS_z$; y and z values at different x values are obtained from Table 1.

estimated to be incorporated into the films, as is tabulated in Table 2. The higher incorporation efficiency of selenium can be ascribed to the lower volatility of selenium compared to sulfur. It should be also noted that an error range of about 1 atomic %, which is a typical value for EDX measurements, will change the values of incorporation efficiency by around 10% in the above calculation.

The observed effects of molecular species on the incorporation efficiency of sulfur into $CuIn(Se,S)_2$ films can be rationalized in the following manner. The chalcogen (Se + S) to metal (Cu + In) ratio is 1.33:1 in the mixed $[Cu_6S_4]^{2-}$ and $[In_2(Se,S)_4]^{2-}$ precursor solution while the ratio in the films is 1:1. Therefore, sulfur from $[Cu_6S_4]^{2-}$ competes with sulfur and selenium from $[In_2(Se,S)_4]^{2-}$ to incorporate into the films. It has been demonstrated through thermogravimetric analysis that $[Cu_6S_4]^{2-}$ is relatively unstable during heat treatment compared with $[In_2Se_4]^{2-}$.[23,24] $[Cu_6S_4]^{2-}$ ions present in a hydrazine solution convert to Cu_7S_4 sheets by losing sulfur while drying at room temperature and lose additional sulfur to form Cu_2S at temperatures below 120 °C.[14,23] In contrast, the indium chalcogenide complex is quite stable, losing minimal amounts of chalcogen below 220 °C, at which point the $CuIn(Se,S)_2$ phase will already be forming in hydrazine-processed films.[14,19,24] Thus, it can be assumed that the Cu−S interactions in $[Cu_6S_4]^{2-}$ ions are significantly weaker than the In−Se or In−S interactions present in the $[In_2(Se,S)_4]^{2-}$ precursor. The disruption of Cu−S bonds would produce free sulfur atoms or volatile derivatives such as ammonium or hydrogen sulfide, which would contribute to the rapid loss of the sulfur. In addition, the size of copper atoms is much smaller than that of indium atoms, so that copper diffusion is likely to dominate in the precursor film,[25] thus leaving sulfur behind to evaporate out during the formation of the $CuIn(Se,S)_2$ phase. This is one possible explanation for the observation that chalcogen species in the $[In_2(Se,S)_4]^{2-}$ precursor are able to more effectively incorporate into the annealed films.

To demonstrate the effects of indium precursor formulation on the electronic properties of the $CuIn(Se,S)_2$ phase, steady state PL measurements were employed to estimate the band gap of $CuIn(Se,S)_2$ films deposited using different types of precursor solution. The recorded data is shown in Figure 5. The main peak of each spectrum, showing near band edge emission, is located at 1.03, 1.09, and 1.14 eV for Type I, II, and III films, respectively. These values are consistent with the empirically determined relationship between band gap energy and sulfur content in the $CuIn(Se,S)_2$ material system.[26]

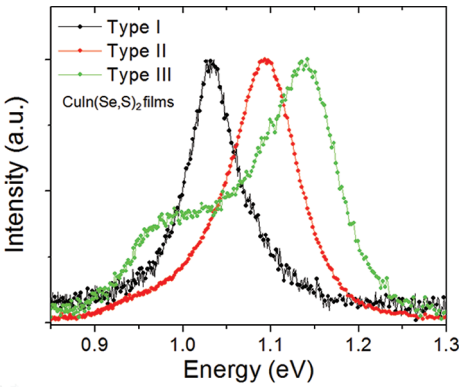

Figure 5. Photoluminescence spectra of $CuIn(Se,S)_2$ films prepared using the three different types of $CuIn(Se,S)_2$ precursor solution.

CONCLUSIONS

In summary, we have developed a simple and reliable description of sulfur and selenium incorporation from their soluble precursor compounds into $CuIn(Se,S)_2$ films. Sulfur values of over 16.3 atomic %, which corresponds to roughly a 33% displacement of selenium by sulfur in the $CuIn(Se,S)_2$ phase, have been demonstrated, and they have produced a corresponding band gap of up to 1.14 eV. This value agrees well with the average band gap of roughly 1.15 eV typically employed in high efficiency $Cu(In,Ga)Se_2$ devices.[27] The facile adjustment of the absorber band gap within a range quite close to its ideal value makes the use of $[In_2Se_{4-x}S_x]^{2-}$ precursors highly relevant to the fabrication of high performance $CuIn(Se,S)_2$ photovoltaic devices.

Through the compositional analysis of films formed using different precursor compositions and ratios, we have determined that sulfur in the $(N_2H_5)_2S$ precursor is too volatile to effectively incorporate into the growing $CuIn(Se,S)_2$ phase. Sulfur from the $[Cu_6S_4]^{2-}$ complex is forced to compete with chalcogen from $[In_2(Se,S)_4]^{2-}$ to incorporate into the films because the chalcogen content in the molecular precursor solution is necessarily larger than that in the films. Approximately 40% of the sulfur atoms from $[Cu_6S_4]^{2-}$ appear to incorporate into the annealed films while approximately 80% of the sulfur and 90% of the

dx.doi.org/10.1021/cm201827c |Chem. Mater. 2011, 23, 4941–4946

selenium atoms from the $[In_2(Se,S)_4]^{2-}$ precursor are successfully incorporated. The higher volatility of the sulfur atoms in $[Cu_6S_4]^{2-}$ compared to that of those in $[In_2(Se,S)_4]^{2-}$ can possibly be ascribed to the lower thermal stability of the $[Cu_6S_4]^{2-}$ complex, as compared with $[In_2(Se,S)_4]^{2-}$. Controlling the composition of the $[In_2Se_{3+x}S_{1-x}]^{2-}$ precursor in the mixed $CuIn(Se,S)_2$ precursor solution offers a reliable mechanism through which to control the sulfur content of the resulting semiconductor material, which, in turn, can enable the precise adjustment of the band gap of hydrazine processed $CuIn(Se,S)_2$ thin films.

AUTHOR INFORMATION

Corresponding Author

*Tel: (310) 825-4052. Fax: (310) 825-3665. E-mail: yangy@ucla.edu.

ACKNOWLEDGMENT

The authors would like to express their gratitude for the generous financial support of EMD Chemicals.

REFERENCES

(1) Zhang, S. B.; Wei, S.-H; Zunger, A. *Phys. Rev. B* **1998**, *57*, 9642.
(2) Repins, I.; Contreras, M. A.; Egaas, B.; DeHart, C.; Scharf, J.; Perkins, C. L.; To, C.; Noufi, R. *Prog. Photovoltaics* **2008**, *16*, 235.
(3) Kapur, V. K.; Bansal, A.; Le, P.; Asensio, O. I. *Thin Solid Films* **2003**, *431−432*, 53.
(4) Kaelin, M.; Rudmann, D.; Tiwari, A. N. *Sol. Energy* **2004**, *77*, 749.
(5) Kaelin, M.; Rudmann, D.; Kurdesau, F.; Zogg, H.; Meyer, T.; Tiwari, A. N. *Thin Solid Films* **2005**, *480−481*, 486.
(6) Hibberd, C. J.; Chassaing, E.; Liu, W.; Mitzi, D. B.; Linco, D.; Tiwari, A. N. *Prog. Photovoltaics* **2010**, *18*, 434.
(7) Todorov, T.; Mitzi, D. B. *Eur. J. Inorg. Chem.* **2010**, *2010*, 17.
(8) Habas, S. E.; Platt, H. A. S; van Hest, M. F. A. M; Ginley, D.S . *Chem. Rev.* **2010**, *110*, 6571–6594.
(9) Mitzi, D. B.; Todorov, T. K.; Gunawan, O.; Yuan, M.; Cao, Q.; Liu, W.; Reuter, K. B.; Kuwahara, M.; Misumi, K.; Kellock, A. J.; Chey, S. J.; Monsabert, T. G.; Prabhakar, A.; Deline, V.; Fogel, K. E. *IEEE Photovoltaic Spec.Conf., 35th* **2010**, 640.
(10) Milliron, D. J.; Mitzi, D. B.; Copel, M.; Murray, C. E. *Chem. Mater.* **2006**, *18*, 587.
(11) Mitzi, D. B.; Yuan, M.; Liu, W.; Kellock, A. J.; Chey, S. J.; Deline, V.; Schrott, A. G. *Adv. Mater.* **2008**, *20*, 3657.
(12) Mitzi, D. B.; Yuan, M.; Liu, W.; Kellock, A. J.; Chey, S. J.; Gignac, L.; Schrott, A. G. *Thin Solid Films* **2009**, *517*, 2158.
(13) Liu, W.; Mitzi, D. B.; Yuan, M.; Kellock, A. J.; Chey, S. J.; Gunawan, O. *Chem. Mater.* **2010**, *22*, 1010.
(14) Chung, C.-H.; Li, S.-H.; Lei, B.; Yang, W.; Hou, W. W.; Bob, B.; Yang, Y. *Chem. Mater.* **2011**, *23*, 964.
(15) Watanabe, I.; Yamamoto, T. *Jpn. J. Appl. Phys.* **1985**, *24*, 1282.
(16) Uhl, W.; Graupner, R.; Reuter, H. *J. Organomet. Chem.* **1996**, *523*, 227.
(17) Weszka, J.; Daniel, Ph.; Burian, A.; Burian, A. M.; Nguyen, A. T. *J. Non-Cryst. Solids* **2000**, *265*, 98.
(18) Landry, C. C.; Lockwood, J.; Barron, A. R. *Chem. Mater.* **1995**, *7*, 699.
(19) Hou, W. W.; Bob, B.; Li, S.-H.; Yang, Y. *Thin Solid Films* **2009**, *517*, 6853.
(20) Tanino, H.; Maeda, T.; Fujikake, H.; Nakanishi, H.; Endo, S.; Irie, T. *Phys. Rev. B* **1992**, *45*, 13323.
(21) Rincon, S.; Ramirez, F. J. *J. Appl. Phys.* **1992**, *72*, 4321.
(22) Bacewicz, R.; Gqbicki, W.; Filipowicz, J. *J. Phys.: Condens. Matter* **1994**, *6*, L777.
(23) Mitzi, D. B. *Inorg. Chem.* **2007**, *46*, 926.
(24) Mitzi, D. B.; Copel, M.; Chey, S. J. *Adv. Mater.* **2005**, *17*, 1285.
(25) Chung, C.-H.; Kim, S. D.; Kim, H. J.; Adurodija, F. O.; Yoon, K. H.; Song, J. *Solid State Commun.* **2003**, *126*, 185.
(26) Neff, H.; Lange, P; Fearheiley, M. L.; Bachmann, K. J. *Appl. Phys. Lett.* **1985**, *47*, 1089.
(27) Repins, I.; Glynn, S.; Duenow, J.; Coutts, T. J.; Metzger, W. K.; Contreras, M. A. *Proc. SPIE, Thin Film Solar Tech.* **2009**, 7409.

NOTE ADDED AFTER ASAP PUBLICATION

This article was published ASAP on October 17, 2011, with an error in eq 3. The corrected version was published ASAP on October 19, 2011.